Aquaculture 530 (2021) 735746

Contents lists available at ScienceDirect

Aquaculture

journal homepage: www.elsevier.com/locate/aquaculture

TEMPO-oxidized biodegradable bacterial cellulose (BBC) membrane coated with biologically-synthesized silver nanoparticles (AgNPs) as a potential antimicrobial agent in aquaculture (*In vitro*)

Sivaramasamy Elayaraja[a,b,d,**], Gang Liu[a], Kamil Zagorsek[b], Mahmoud Mabrok[c,d], Mingdong Ji[a], Zhangying Ye[a], Songming Zhu[a,*], Channarong Rodkhum[d,*]

[a] College of Biosystems Engineering and Food Sciences, Zhejiang University, Hangzhou 310058, China
[b] Technical University of Liberec, Liberec 46117, Czech Republic
[c] Department of Fish Diseases and Management, Faculty of Veterinary Medicine, Suez Canal University, Egypt
[d] Fish Infectious Diseases Research Unit (FID RU), Department of Veterinary Microbiology, Faculty of Veterinary Science, Chulalongkorn University, Bangkok 10330, Thailand

ARTICLE INFO

Keywords:
Pseudomonas sp.
AgNPs
BBC membrane
Aquatic pathogens
Bactericidal activity

ABSTRACT

The emergence of drug-resistance pathogens is one of the major challenges in aquaculture. Finding an alternative remedy for diseases control is now crucial and indispensable. The present study aimed to develop different silver nanocomposite BBC membranes and verified their bactericidal activity either synergistically or independently against seven threatening aquatic pathogens (*Vibrio harveyi, V. parahaemolyticus, V. alginolyticus, V. vulnificus, Aeromonas hydrophila, A. veronii* and *Streptococcus iniae*) using membrane disc diffusion and antibacterial log reduction assays. The aqueous extract of *Pseudomonas* sp. was used for the synthesis of AgNPs and the composite BBC materials were characterized using FTIR, XRD, EDS, and FESEM to confirm their holding capacity of integrated AgNPs. Results evidenced that the TEMPO-oxidized BBC membrane coated with bacterial-based AgNPs exhibited an excellent crystallinity, porous properties, and strongest holding capacity. The membrane also showed potent bactericidal activity represented by wide inhibitory zones (17–20 mm), high killing ratios (95.93–99.86%). and high antibacterial log-reduction values (1.39–2.85). In conclusion, the synergism between TEMPO-oxidized BBC membrane and biologically synthesized AgNPs is an eco-friendly alternative remedy to control aquatic diseases without serious impact.

1. Introduction

Aquaculture is one of the most promising fish-producing sectors that can cover the gap of food shortage due to overpopulation worldwide (FAO, 2018). The sustainability of this sector is limited by the increased incidence of myriad diseases, induced by several opportunistic pathogens including bacteria, fungi, and virus (Lightner, 1985; Surachetpong et al., 2017; Austin, 2019; Gholipourkanani et al., 2019). The most common crisis in aquaculture is mainly caused due to bacterial infection (Toranzo et al., 2005; Mabrok et al., 2016), mainly Vibrionacea (El-Sayed et al., 2019; Xu et al., 2019; Zhang et al., 2020), *Aeromonas hydrophila* (Algammal et al., 2020), *A. veronii* (Dong et al., 2017), and *Streptococcus iniae* (Agnew and Barnes, 2007). Although, the classical antibiotic treatments can destroy or inhibit most of the aquatic threatening pathogens; their indiscriminate use becomes completely inadmissible due to the influence of emerging drug-resistant pathogens (Bernal et al., 2017; Wahdan et al., 2020). To the best of our knowledge, there were no proper and/or effective alternative remedies for the treatment of these pathogens in aquaculture. Accordingly, still, researchers are extensively working to find potential antimicrobial biomaterials that can overcome the current issues.

Among various biomaterials, the potential ions (Ag, Au and chitosan) composite biodegradable bacterial cellulose (BBC) material is considered as an excellent one with potent antimicrobial properties (Kumar et al., 2020). BBC has been extensively used in biomedical sciences, tissue engineering, wound dressings, and drug delivery (Wu et al., 2014; Khamrai et al., 2017). Recent studies were reported on molecular structure and physical characterization of BBC membrane,

* Corresponding authors.
** Corresponding author at: College of Biosystems Engineering and Food Sciences, Zhejiang University, Hangzhou 310058, China; Fish Infectious Diseases Research Unit (FID RU), Department of Veterinary Microbiology, Faculty of Veterinary Science, Chulalongkorn University, Bangkok 10330, Thailand.
E-mail addresses: elayabact@yahoo.com (S. Elayaraja), zhusm@edu.cn (S. Zhu), channarong_r@yahoo.com (C. Rodkhum).

https://doi.org/10.1016/j.aquaculture.2020.735746
Received 9 April 2020; Received in revised form 16 July 2020; Accepted 18 July 2020
Available online 22 July 2020

including thermal and mechanical stability, flexibility, nontoxicity (Pal et al., 2017), crystallinity, durability, water retention capacity (Oliveira et al., 2018), and strong biocompatibility (Rajwade et al., 2015). BBC membrane is produced simply by Acetobacter bacteria (*Gluconacetobacter* sp.) and its purity is relatively high compared to plant cellulose membrane (Feng et al., 2014). The antimicrobial activity of BBC membrane can be increased by integrating BBC membrane with oxidizing agents (TEMPO) and some potential guest ions nanoparticles (NPs) such as silver nitrate ($AgNO_3$) (Abdel Rahim et al., 2017; Elayaraja et al., 2017), silver chloride (AgCl) (Hu et al., 2009), zinc (Zn) (Wasim et al., 2020), titanium (Ti) (Gutierrez et al., 2013), copper oxide (CuO) (Vasantharaj et al., 2019) and gold (AuNPs) (Chen et al., 2015).

TEMPO-mediated oxidation is the most valuable method for cellulose activation since it is a backbone for introducing functional carboxyl groups (Feng et al., 2014; Elayaraja et al., 2017). Besides, TEMPO acts as a binding device that promotes the formation of aldehyde-carboxyl group complex to reduce and stabilize the cellulose template for AgNPs incorporation eco-friendly (Lai et al., 2014).

Silver composite BBC materials are widely used as one of the most promising potential biomaterials (Adepu and Khandelwal, 2018; Loh et al., 2018). BBC nanocomposite has unique optic and catalytic features to create new and advanced functional materials (Elayaraja et al., 2017). The impact of this material is related but not limited to their bactericidal activities (Singh et al., 2015). The bactericidal function is due to the release of silver ion (Ag^+) during the elemental process of silver compounds in aqueous solution. AgNPs can also serve as a means of more efficient delivery of Ag^+ to bacteria cytoplasm and membrane (Xiu et al., 2012) through several patterns such as interacting with DNA, respiratory chain, and cell division (Mijnendonckx et al., 2013; Pourali et al., 2014).

Indeed, the chemically synthesized AgNPs tend to hold some chemical impurities after completing the reaction (Balashanmugam and Kalaichelvan, 2015; Saha and Gupta, 2017), and thus could induce unfavorable toxicity in various medical and pharmaceutical applications. Moreover, the preparation of chemically synthesized AgNPs ultimately needs restricted physical conditions such as high pressure, high energy and variable temperature (Mitiku and Yilma, 2018). In contrast, AgNPs of bacterial origin are clean, non-toxic, eco-friendly, environmentally benign synthetic procedure, and have a strong bactericidal activity (Sivaramasamy et al., 2016). Hence, there is an ever-growing need to use these products as a surrogate for other chemical and physical AgNPs (AbdelRahim et al., 2017). Recently, several approaches have been developed to synthesize inorganic nano-and micro materials based on the use of microbes (Mandal et al., 2006). Among them, *Pseudomonas* sp., has received great attention in the biosynthesis of NPs due to its rapid growth, ease of handling, and genetic stability (Singh et al., 2018). Extracellular synthesis of microbial-based nanoparticles has been mediated by various enzymatic reactions, where the nitrate reductase enzyme can promote the releasing and elimination of metal nanoparticles from the metal ions (Nelson et al., 2005). In view of the above information, the objective of this study was to prepare different silver nanocomposite BBC membranes and to investigate their bactericidal activity either synergistically or independently against different threatening aquatic pathogens using membrane disc diffusion and antibacterial log reduction assays.

2. Materials and methods

2.1. Bacterial isolates and culture conditions

To prepare BBC membrane and bacterial-based AgNPs, two species of bacteria *Gluconacetobacter xylinum*, and *Pseudomonas* sp. were kindly provided by China general microbiological culture collection centre (Beijing, China) with a reference preservation code of CGMCC NO 1.2378 and 9651, respectively. *Gluconacetobacter xylinum* was routinely cultured on Schenk and Hildebrandt (SH) medium (Schenk and Hildebrandt, 1972), containing glucose 20 g/L, tryptone 5 g/L, yeast extract 5 g/L, Na_2HPO_4 .$12H_2O$ 2.7 g/L, citric acid 1.5 g/L, agar 15 g/L with pH 5.0 at 30 °C in a shaking incubator (120 rpm) for 5 days, whereas the *Pseudomonas* sp. were cultured on *Pseudomonas* base agar at 37 °C for 24 h. Both bacteria were kept frozen at −20 until used for further examination.

For the bactericidal assay, the seven pathogens (*Vibrio harveyi, V. parahaemolyticus, V. alginolyticus, V. vulnificus, Aeromonas hydrophila, A. veronii,* and *Streptococcus iniae*) were selected, which were previously isolated from the skin tissues and internal organs of diseased shrimp (*Penaeus vannamei*) and Nile tilapia (*Oreochromis niloticus*). The pathogens were identified using different sets of biochemical reagents and were confirmed by API 20E identification kits. The chemical reagents were purchased from Macklin Biochemical Co. Ltd. (Shanghai, China) and Luoyang biotechnology co. LTD (Hangzhou, China). Further molecular characterization was performed using one set of universal primers targeting 16 s rRNA gene (27F, 5-AGAGTTTGATCCTGGCTCAG-3 and 1492R, 5-CTACGGCTACCTTGTTACGA-3), where the species identity was confirmed by 16 s rDNA sequencing and sequence alignment using NCBI basic Local alignment search tool. These bacteria were routinely cultured on Tryptic soy agar (TSA) overnight at 28 °C. The harvested colonies were checked for their purity and then inoculated into 5 mL of fresh sterile Tryptic soy broth (TSB) and/or nutrient broth (NB) for an additional 24 h at 250 rpm and 28 °C. The bacteria are kept frozen at −20 °C until used for further examinations.

2.2. Preparation of BBC membrane

The BBC membrane was prepared from *G. xylinum*1.2378 bacteria using the methods described by Elayaraja et al. (2017). Briefly, the bacteria were grown in Schenk and Hildebrandt (SH) medium under the same optimal conditions described above. A single pure colony was harvested and inoculated into 50 mL of SH broth at 30 °C in a shaking incubator (120 rpm) for 24 h. The culture was centrifuged (Thermo-Fisher Scientific, Fiberlite F20-6 × 100) at 10864 ×*g* for 15 min and 10 mL of the collected supernatant was then mixed with 100 mL of SH broth in 500 mL Erlenmeyer flask at 30 °C for 10 days. The BBC membrane (wet weight 14.7 g, and 8.1 cm) was collected aseptically from the surface of the mixture, purified at 100 °C for 1 h, and then treated with 0.1 M NaOH to eliminate any bacterial cells and residues. The collected BBC membrane was further washed with deionized water until obtaining a neutral pH. Eventually, the BBC membrane was subjected to three different processes: (i) TEMPO-oxidized BBC membrane coated with (pure $AgNO_3$) NPs (chemical composite BBC, CC-BBC), (ii) BBC membrane coated with bacterial-based AgNPs (biological composite BBC, BC-BBC), and (iii) TEMPO-oxidized BBC membrane coated with bacterial-based AgNPs (chemico-biologically composite BBC, CBC-BBC).

2.3. TEMPO-mediated oxidation process (chemical process)

The carboxyl groups (backbone) of BBC membrane were oxidized using 2,2,6,6-tetramethylpiperidine-1-oxyradical (TEMPO) according to the method described by Cao et al. (2013). Briefly, 0.016 g of TEMPO was dissolved in 90 mL of sodium phosphate buffer (0.1 M, pH 6.8) in a tight flask. Subsequently, 1.13 g of sodium chloride was added to the mixture to accelerate the oxidation process.

2.4. Integration of AgNPs into the oxidized BBC membrane (CC-BBC)

It was performed according to the method described by Cao et al. (2013). Briefly, the oxidized BBC membrane was immersed in 50 mL of an aqueous solution of silver nitrate ($AgNO_3$) at a final concentration of 1 mM and pH 6 without adding reducing agents and left incubated overnight at 40 °C in a dark place. The immersed membrane was further

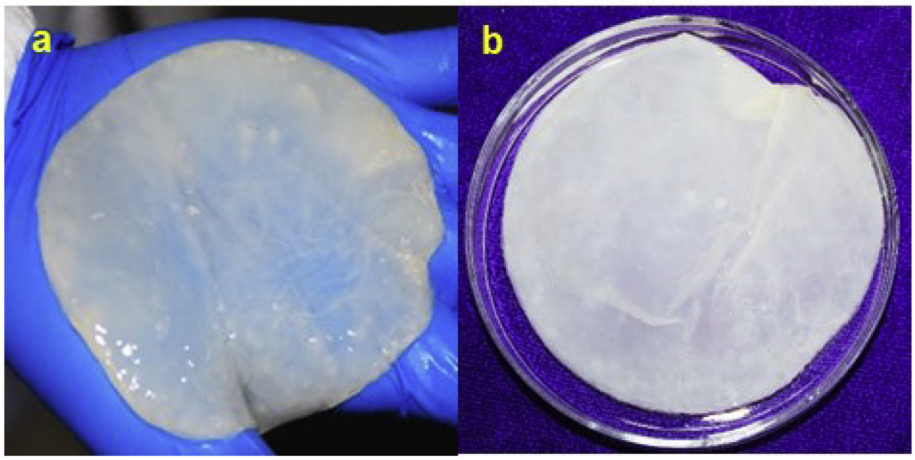

Fig. 1. Biodegradable bacterial cellulose (BBC) membrane formed by *G. xylinum*. (a) collected BBC membrane before wash; (b) BBC membrane after washing with deionized water.

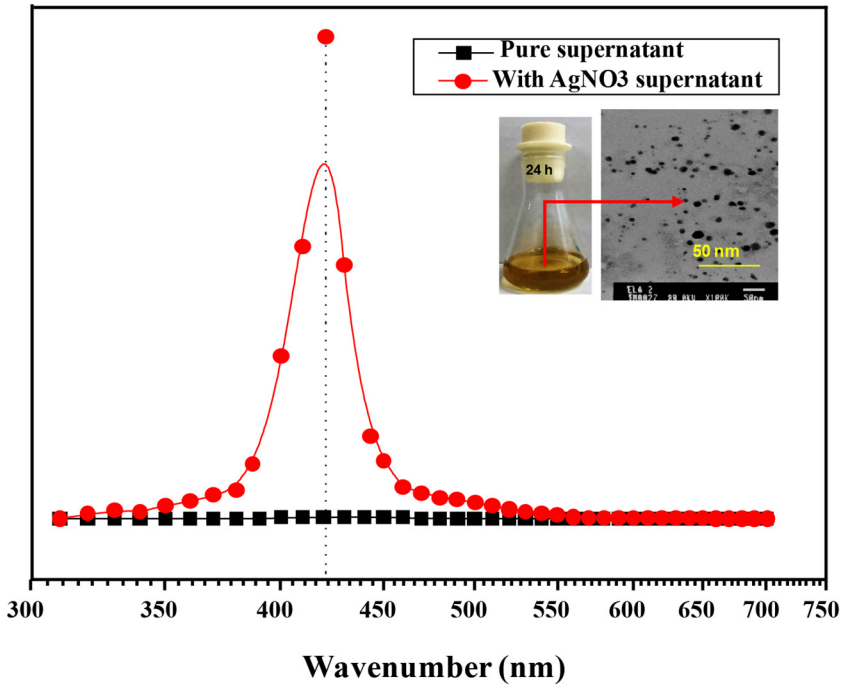

Fig. 2. UV–Vis spectra of AgNPs, produced from the extracellular products of *Pseudomonas* sp. Inset TEM image represented the size (50 nm magnification) and distribution of AgNPs particles.

purified using deionized water. The final product (AgNPs- TEMPO-oxidized BBC) was successfully characterized and used for the further antibacterial assay.

2.5. Preparation of AgNPs from the extracellular products of Pseudomonas sp. (biological process)

It was prepared according to the method described by Vanaraj et al. (2017) with slight modifications. In brief, the *Pseudomonas* sp. was cultured on Pseudomonas base agar under the same conditions described above. After cultivation, the supernatant was obtained by centrifugation (ThermoFisher Scientific, Fiberlite F20-6 × 100) at 15644 ×*g* for 10 min, and 100 mL of the supernatant was filtered through a 0.45-μm syringe filter (PVDF,25pcs/Lot, Lab Chemical Labware, China) and mixed with a filter-sterilized solution of $AgNO_3$ (99.9% pure) to reach the final concentration of 1 mM, pH 7. The mixture was then incubated in a dark condition at 30 °C and 200 rpm and was analyzed at 300–700 nm from 6 h to 36 h using a UV–Vis Spec. (Ultraviolet-visible spectroscopy, Agilent Technology–G6860A, Cary 60) to confirm the production of AgNPs. Filtered supernatant without $AgNO_3$ was used as a blank. The reduction of silver ions (Ag +) was monitored by visual observation for the synthesized nanoparticles according to the method of Velmurugan et al. (2014). AgNPs were confirmed by UV–Vis and their sizes and shapes were determined using carbon-coated copper grids and visualized under transmission electron microscopy (TEM, JEOL-JEM-1200 EX model).

2.6. Concentration and conversion calculation of Ag^+ to AgNPs (Ag^0) by ICP-AES

The concentration of AgNPs (Ag^0) after the synthesis process, either biological or chemically was determined using inductively coupled plasma atomic emission spectroscopy (ICP-AES, Shimadzu ICPE-9820, CCD detector, Japan) according to Rahman et al. (2019). Briefly,

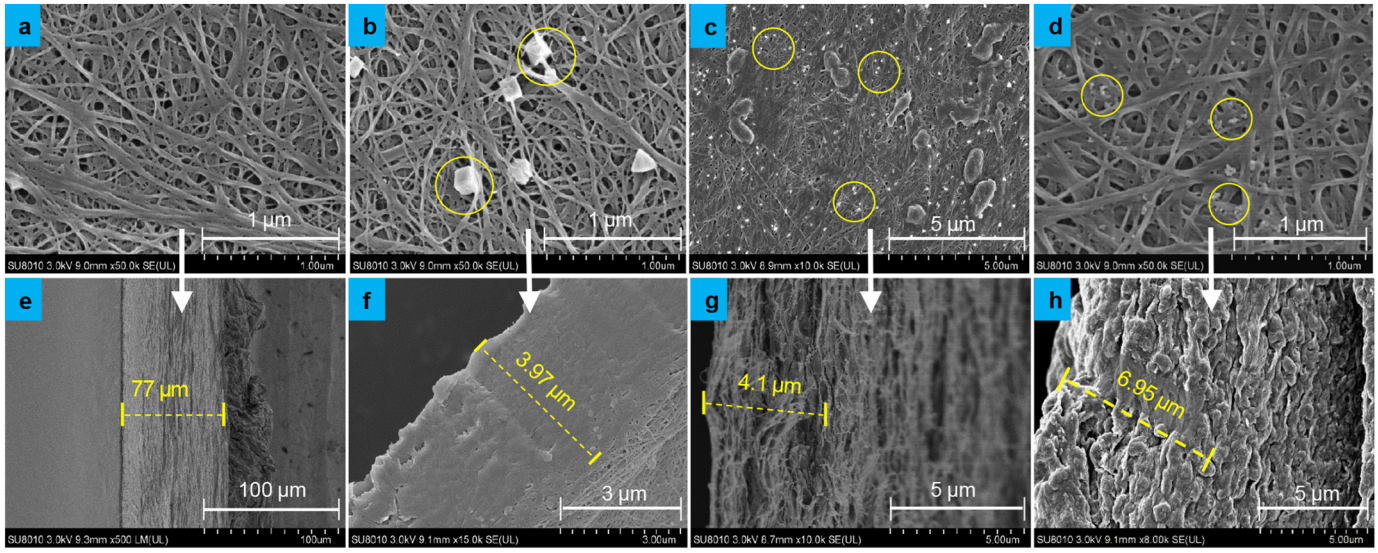

Fig. 3. Field-Emission Scanning Electron Microscopy (FESEM) analyses of pure and treated AgNPs-based BBC membranes. (a, e) pure BBC membrane; (b, f) TEMPO-oxidized BBC membrane coated with pure silver NPs (CC-BBC membrane); (c, g) BBC membrane coated with bacterial-based AgNPs (BC-BBC membrane); (d, h) TEMPO-oxidized BBC membrane coated with bacterial-based AgNPs (CBC-BBC membrane). e, f, g, and h showed the cross-section and diameter of each membrane. Yellow circles donate variable sizes of synthesized AgNPs at different scales bar among the BBC membranes, while the dot lines clarified the diameter size of such membrane. (For interpretation of the references to colour in this figure legend, the reader is referred to the web version of this article.)

suitable volumes of the overnight mixture of synthesized AgNPs were 20× diluted with 5% nitric acid solution (HNO3) and analyzed to assess the total amount of silver. NaCl (1 mM) was added to the diluted samples and incubated for 12 h to precipitate the untreated Ag + as AgCl. The samples were then centrifuged at 1000 ×*g* for 10 min to remove the precipitated salt and the supernatant was 20× diluted with 5% nitric acid solution for ICP-AES analysis. An equal volume of Nitric acid solution (5%) in Elix water was used as a blank and the detection of Ag was at a wavelength of 328.068 nm. Each sample was analyzed in triplicates, where the concentration of Ag in the supernatants represented the amount of released AgNPs that were not precipitated by NaCl.

The conversion efficiency (C%) of AgNPs was calculated as a percentage using the following formula:

$$C\% = A/B \times 100$$

where A is the concentration of the released AgNPs (mM) and B is the initial concentration of $AgNO_3$ used for the synthesis process (1 mM).

2.7. Integration of bacterial-based AgNPs into the pure BBC membrane (BC-BBC membrane)

The purified BBC membrane was immersed into 100 mL of extracellular AgNPs solution and incubated at 37 °C for 24 h at 200 rpm. The immersed membrane was rinsed with deionized water to remove excess $AgNO_3$ solution. Finally, the BBC was freeze-dried for further characterization and antibacterial assay.

2.8. Integration of bacterial-based AgNPs into the TEMPO-oxidized BBC membrane (CBC-BBC membrane)

The TEMPO-oxidized membrane was immersed into 100 mL of biologically synthesized AgNPs solution and incubated at 37 °C and 200 rpm for 24 h. The immersed membrane was rinsed with deionized water to remove the excess of $AgNO_3$ solution. Finally, the BBC was freeze-dried for further characterization and antibacterial assay.

2.9. Characterization of different modified BBC membranes

2.9.1. Field emission scanning Electron microscopy (FESEM)

The entire structure and surface morphology of different modified membranes were investigated by FESEM (SU8010, Hitachi High-Technology Corporation, Japan), while the distribution patterns of integrated AgNPs within the membranes were observed by energy-dispersive X-ray spectroscopy (EDS).

2.9.2. Fourier transform infrared (FTIR)

FTIR analysis of the dried and grounded BBC membranes was performed on Avatar 370, Termmo Nicolet (USA), using samples prepared as KBr pellets. The spectra of the samples were collected over the range of 4000–400 cm^{-1} with a resolution of 4 cm^{-1}.

2.9.3. X-ray diffraction (XRD)

The crystallinity of the BBC membranes was investigated using x-ray step-scanning powder diffractometer (XRD, PANalytical, X'Pert PRO, Netherland). The BBC membranes were mounted on a copper holder and scanned in 2θ (10^o-40^o) Bragg-Brentano geometry using Cu-Kα radiation (K = 1.54 Ao) at a scanning rate of 0.5/min, using a voltage of 30 kV and a current of 20 mA.

2.10. Antibacterial assay

The antibacterial activities of the pure and treated BBC membranes were evaluated against various aquatic pathogens. For the preparation of inoculum, all bacterial cultures were adjusted to a final concentration of 10^7 colony-forming unit (CFU/mL) using a classical plating technique and by mean of Helber counting chamber. The antibacterial assay was performed using a membrane disc diffusion and log-reduction assays according to Feng et al. (2014) and Yang et al. (2012), respectively with some modifications. Briefly, for a membrane disc diffusion method, pure and treated BBC membranes were cut into uniform flat discs with of 5–6 mm diameter and sterilized both the side under UV for 1 h. The disc was placed aseptically on different plates of Mueller-Hinton agar, seeded with different bacteria at a concentration of 10^7 CFU/mL. The plates were incubated at 28 °C for 18 h and were examined for zones of inhibition.

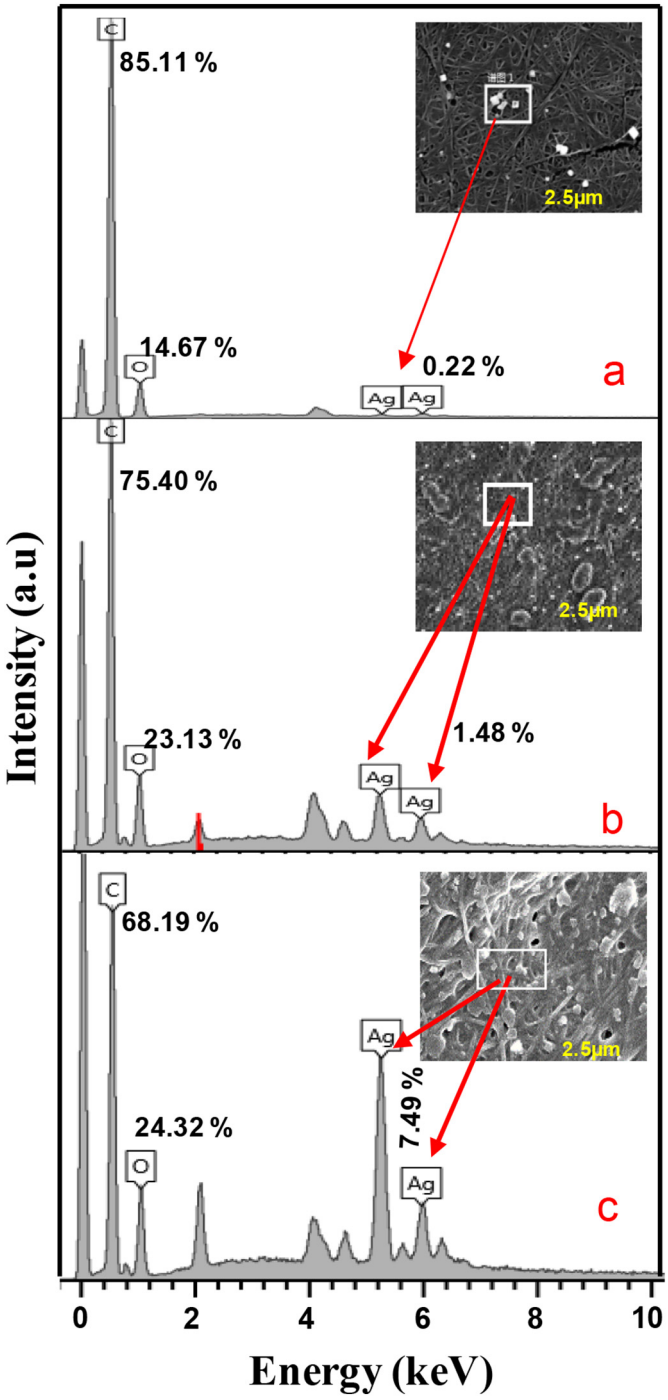

Fig. 4. Energy-dispersive X-ray (EDX) spectroscopy for elemental analysis of treated AgNPs-based BBC membranes. (a) TEMPO-oxidized BBC membrane coated with AgNPs (CC-BBC membrane); (b) BBC membrane coated with bacterial-based AgNPs (Biological BC-BBC membrane); (c) TEMPO-oxidized BBC membrane coated with bacterial-based AgNPs (CBC-BBC membrane).

Regarding the log-reduction assay, it was used for quantitatively to evaluate the antimicrobial activity of differently treated nanocomposite BBC membranes. Briefly, 100 μL of each bacterial suspension was transferred onto the treated membranes and incubated for18h under complete aseptic condition. Subsequently, the streaked membranes were washed off using 50 mL of PBS (0.03 M) to harvest the bacteria. Serial dilutions of harvested bacteria were then cultured on tryptic soy agar at 37 °C for 24 h for counting. The results were expressed as CFUs. The same procedure was performed on a pure BBC membrane without AgNPs addition and served as a control. The antimicrobial activity of the different treated membranes was assessed using different equations (Pinto et al., 2009).

Bactericidal activity

$$= \text{Log CFU } T_0 \text{ control} - \text{Log CFU } T_{18} \text{ nanocomposite BBC membrane.}$$

Bacteriostatic activity

$$= \text{Log CFU } T_{18} \text{ control} - \text{Log CFU } T_{18} \text{ nanocomposite BBC membrane.}$$

Killing ratio (%)

$$= \frac{\text{CFU } T_{18} \text{ control–CFU } T_{18} \text{ nanocomposite BBC membrane} \times 100.}{\text{CFU } T_{18} \text{ control.}}$$

CFU T_0 control and CFU T_{24} control purposed the viable bacterial number for the pure membrane (control) at 0 h and 24 h of incubation, respectively, while CFU T_{24} nanocomposite BBC membrane meant the viable bacterial number for the treated nanocomposite membrane at 24 h of incubation.

2.11. Statistical analysis

It was performed using SPSS statistics 20.0 for windows package (IBM Corporation, NY, USA). Data are expressed as mean ± standard error of the mean (*SEM*) and were analyzed using one way ANOVA and Student's *t*-test to determine the differences between tested BBC membranes. The level of significance used was $P \leq .05$.

3. Results and discussion

Biodegradable bacterial cellulose membrane is being considered as one of the most promising biomaterials that are being extensively used in the field of biomedical and agricultural science (Pal et al., 2017). Based on our previous study Elayaraja et al. (2017), 3-D nanofibers thick BBC membrane was successfully produced from the extracellular product of *G. xylinum* after 10 days (Fig. 1a) and was subsequently, washed with deionized water, boiled to remove any impurities without any further changes in its physical appearance and stiffness (Fig. 1b). BBC itself does not have any antimicrobial properties to prevent microbial infections (Pourali et al., 2014). Although several studies reported that the basic BBC membrane impregnated with some potential guest ions NPs enhanced the antimicrobial property to increase its beneficial use for diseases control (Xu et al., 2019), there are many limitations on the use of chemically-synthesized BBC membrane in biological application due to the high load of chemical impurities (Pourali et al., 2014; Balashanmugam and Kalaichelvan, 2015). Hence, it is imperative to improve BBC composites with strong antimicrobial NPs of bacterial origin in an eco-friendly manner without having any toxic and carcinogenic properties. The present study aimed to impregnate the bacterial-based AgNPs, produced from *Pseudomonas* sp. extracellular products with an oxidized BBC membrane to find out an alternative remedy to control the bacterial diseases, particularly in aquaculture.

Fig. 2 showed the formation, persistence, and maximum absorption of bacterial-based AgNPs (reddish-brown) at approximately 420 nm. TEM analysis revealed that the nanoparticles were spherical in shape with the size ranged between 5 and 25 nm in diameter. The results are in good agreement with Li et al. (2010) and Pourali et al. (2014). The size and shape of nanoparticles are necessary to produce a nanomaterial with strong antimicrobial activity, as the smallest particles can penetrate and interact easily with bacterial cell walls and thus have better antibacterial activity (Fondevila, 2010).

The concentration of AgNPs at the completion of each synthesis process was measured by ICP-AES and the conversion efficiency was calculated based on these concentrations. In terms of production of Ag^0, the amount of bio-released AgNPs (0.733 mM) was significantly higher

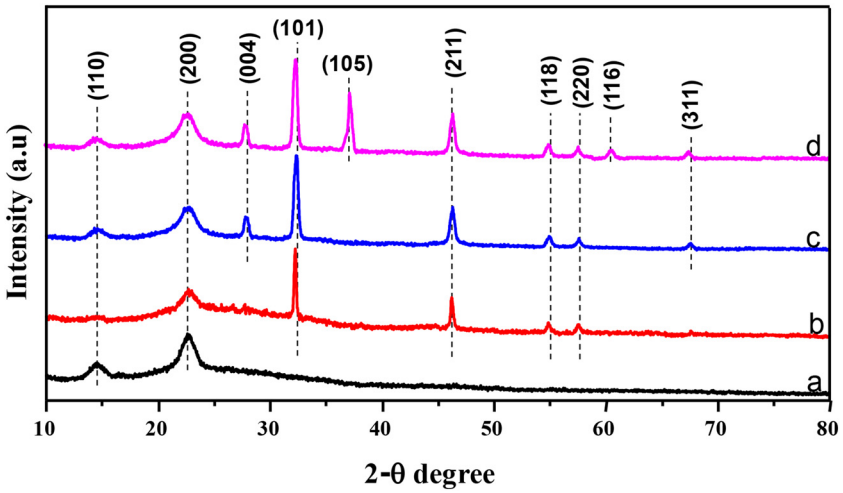

Fig. 5. X-Ray Diffraction (XRD) patterns of pure and treated AgNPs-based BBC membranes. (a) pure BBC membrane; (b) TEMPO-oxidized BBC membrane coated with AgNPs (CC-BBC membrane); (c) BBC membrane coated with bacterial-based AgNPs (BC-BBC membrane); (d) TEMPO-oxidized BBC membrane coated with bacterial-based AgNPs (CBC-BBC membrane).

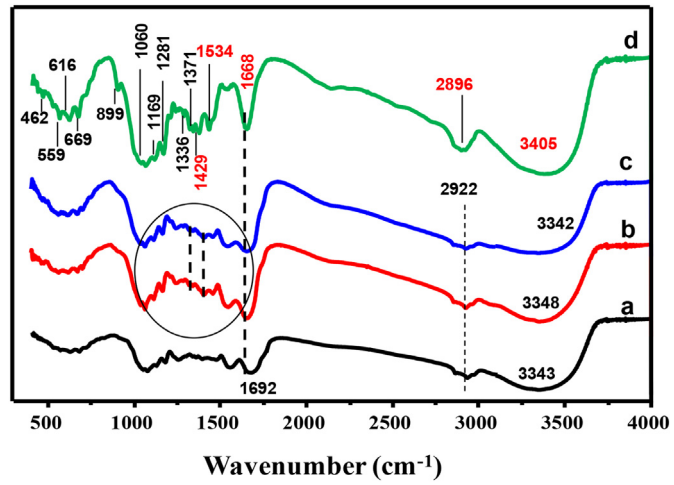

Fig. 6. Fourier-transform infrared (FTIR) spectrum analysis of pure and treated AgNPs-based BBC membranes. (a) pure BBC membrane; (b) TEMPO-oxidized BBC membrane coated with AgNPs (CC-BBC membrane); (c) BBC membrane coated with bacterial-based AgNPs (BC-BBC membrane); (d) TEMPO-oxidized BBC membrane coated with bacterial-based AgNPs (CBC-BBC membrane).

Table 1
Functional groups of FTIR spectra of pure and AgNPs treated BBC membranes.

Peak location (cm^{-1})	a	b	c	d	[a]Functional group
3405–3342	+	+	+	+	Secondary amide (N—H stretch, H-bonded)
2922–2896	+	+	+	+	Alkane (C—H stretching)
1692–1668	+	+	+	+	Carbonyl (C=O)
1534 and 1429	−	−	−	+	Aromatic (C—C stretching)
1371	−	−	−	+	Alkyl Halide (C—F)
1336–1060	−	+	−	+	Primary alcohol (C—O stretching)
899	−	−	−	+	Alkene (=C—H bending
669–462	−	+	+	+	Alkene (=C—H bending)

+, presence of the functional group in the BBC membranes; −, absence of functional group in the BBC membranes; a, pure BBC membrane; b, TEMPO-oxidized BBC membrane coated with AgNPs (CC-BBC membrane); c, BBC membrane coated with bacterial-based AgNPs (BC-BBC membrane); d, TEMPO-oxidized BBC membrane coated with bacterial-based AgNPs (CBC-BBC membrane).

[a] The corresponding functional groups for each peak location.

than that obtained in completing the chemical process (0.479 mM) with a conversion efficiency of 73.3 and 47.9%, respectively. These values are consistent with previous findings from the EDX spectroscopy for elemental analysis (Fig. 4). The respective results are in good agreement with Rahman et al. (2019) who stated that the biosynthesis of AgNPs from wild type and cell wall deficient strains was increased at 1.250 mM concentration of $AgNO_3$ then at 0.625 mM. In addition, the bio-released AgNPs did not reach 100% with the current assay as the higher toxicity of Ag + compared to other mineral precursors could limit the reduction of Ag^+ to Ag^0 facilitated by metabolically produced reducing agents (Shabnam and Pardha-Saradhi, 2013; Dahoumane et al., 2014).

The surface morphology of the four BBC membranes was investigated using FESEM (Fig. 3). The pure BBC membrane (untreated) showed expected nanofibers with well-organized 3D web-like porous of 100 nm (Fig. 3a). The selected BBC has good physical characteristics and better inherent biocompatibility for further studies, consistent with (Rouabhia et al., 2014). Significantly, after oxidation by TEMPO, the membrane became more sophisticated as the surface area was smooth and homogeneous, while the pores showed higher density and irregular distribution, congruent with (Xu et al., 2019). Thus, could be attributed to the TEMPO-mediated oxidation process, in which the hydroxyl groups of BBC membrane were converted to carboxyl and aldehyde functional groups particularly at the C6 position that in turn enhanced the physical properties of the entire pure BBC membrane (Elayaraja et al., 2017; Jun et al., 2019). Similar results were reported by Lai et al. (2014) who stated that TEMPO-oxidized jute fibers showed variable sizes of AgNPs, ranging from 50 ± 2 to 90 ± 4.7 nm in diameter after impregnation in a silver solution.

CC-BBC membrane produced polymorphs AgNPs with an approximate size of 80 nm in diameter with a cubic structure on the surface of the BBC membrane (Fig. 3b). The surface morphology of the BC-BBC membrane showed aggregation and clustering of nanoparticles in different surface areas of the membrane (Fig. 3c). In contrary, the AgNPs were randomly, uniformly dispersed, and strongly adhered to the 3D nanofibers of the CBC-BBC membrane, and thus covering the entire surface of the membrane and also reduced the pore density (Fig. 3d). These results suggested that the TEMPO-oxidized BBC membrane allowed the bacterial-based AgNPs (spherical shape) with an average diameter ranged from 5 to 25 nm to be diffused throughout its inner space in an easier way than the other pure and chemically modified membranes, in agreement with Feng et al. (2014). The cross-section investigation of the internal matrix of BBC membrane using FESEM (Fig. 3e, f, g and h) suggested that the ability of AgNPs to penetrate the internal matrix was noticeably increased in addition to the membrane thickness Fig. 3h. These results are consistent with those reported by Pal et al. (2017).

The spectra map obtained from EDS spectra analysis (Fig. 4a, b, c and inset) (3cps/KeV) showed that the silver elemental peaks were

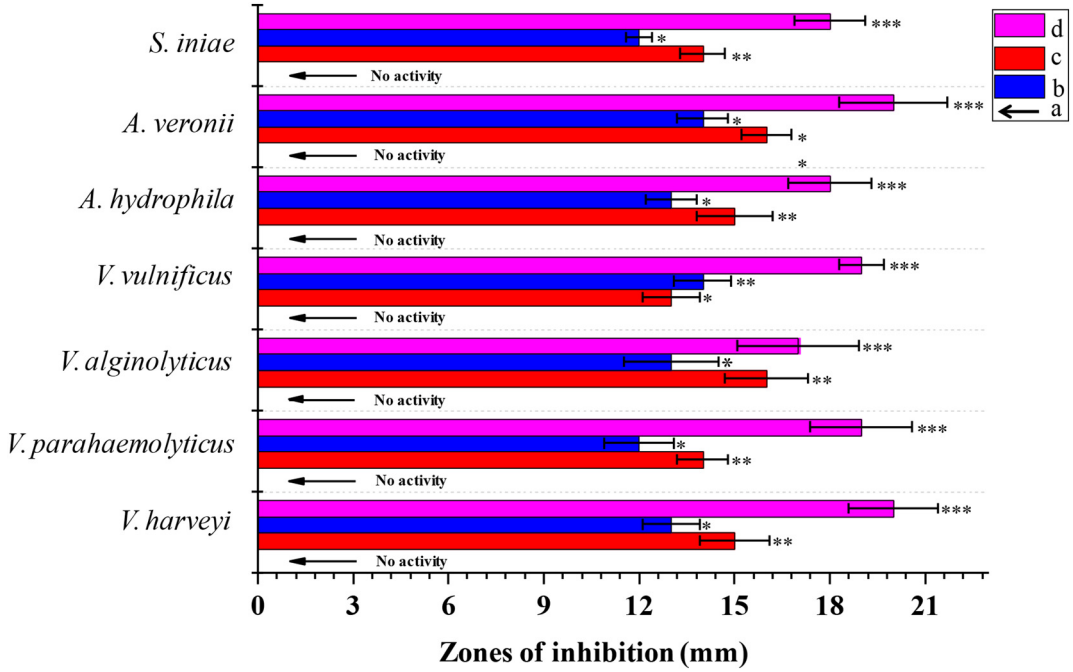

Fig. 7. Zones of inhibition (mm) of seven aquatic threatening pathogens after 18 h incubation with pure and treated AgNPs-based BBC membranes. (a) pure BBC membrane; (b) TEMPO-oxidized BBC membrane coated with AgNPs (CC-BBC membrane); (c) BBC membrane coated with bacterial-based AgNPs (BC-BBC membrane); (d) TEMPO-oxidized BBC membrane coated with bacterial-based AgNPs (CBC-BBC membrane). Data are presented as mean SD ± (n = 3). The level of significance was *$P \leq .05$, **$P \leq .01$, and ***$P \leq .001$ using t-test.

Table 2
Average zones of inhibition (mm) of seven aquatic threatening pathogens after 18 h incubation with TEMPO-oxidized BBC membrane coated with bacterial-based AgNPs (CBC-BBC membrane) using a membrane disc diffusion method.

Tested pathogens	Membrane disc diameter (mm)	Average inhibition zones (mm)
Vibrio harveyi	5–6	20 ± 1.4
Vibrio parahaemolyticus		19 ± 0.6
Vibrio alginolyticus		17 ± 1.9
Vibrio vulnificus		19 ± 1.5
Aeromonas hydrophila		18 ± 1.3
Aeromonas veronii		20 ± 1.1
Streptococcus iniae		18 ± 1.7

Data are presented as mean SD ± (n = 3).

significantly increased in the CBC-BBC membrane with a maximum peak of 7.49% (Fig. 4d). Additionally, two extra elemental peaks (C and O) were observed in the same membrane, which might be from the stabilizing protein of the membrane. These results are inconsistent with those reported by Jinga et al. (2013) and Khan et al. (2015). Surprisingly, the peak reported in this study was relatively lower than that of Elayaraja et al. (2017) who mentioned that silver atoms in the NPs exhibited a strong signal of 73.89%.

Based on XRD patterns, a pure (untreated) BBC membrane showed only two distinct peaks at 14.3° and 22.5° (Fig. 5a), indicating that the membrane was not completely crystalline. The CC-BBC membrane had four additional peaks at 32.6°, 46.3°, 55.1° and 57.8° corresponding to the positions 101, 211, 118, and 220, respectively (Fig. 5b), which indicated the crystallinity of the membrane and ensured the presence of AgNPs cubic structure, in agreement with Wan et al. (2006) and Cao et al. (2013). Regarding BC-BBC membrane, the results showed an additional one strong and one weak peak at 38.2° and 68.7° corresponding to the position 004 and 311, respectively (Fig. 5c). Likewise, the CBC-BBC membrane displayed two extra peaks at 46.1° and 62.3° corresponding to the positions 105 and 311, respectively, when compared with the biologically composite one (Fig. 5d), in agreement with Elayaraja et al. (2017).

Overall, the BC-BBC and CBC-BBC membranes have the strong binding capacity to the eliminated AgNPs and therefore expected to have strong bactericidal activity. Furthermore, the characteristic peaks, shapes, and crystallinity of those membranes may be related to the functional carbon sources, pH, optimum time, and drying method used (Pourali et al., 2014).

The FTIR spectrum was performed to identify the promising interface between AgNPs and BBC composites (Fig. 6). The result revealed that there was a significant variation among each band between 4000 and 400 cm^{-1} and thus revealed the presence of different functional groups (Table 1). In the terminal base, the vibration between 3342 and 3405 cm^{-1} was observed, representing commonly obtained molecule C—H (carboxyl group) and vibration near 2922–2896 cm^{-1} linkages to O—H (hydroxyl) (Pal et al., 2017). Both CC-BBC and BC-BBC membranes exhibited a group of absorption peaks at the wavenumber 1500–1000 cm^{-1} due to the C − O and C − C stretching vibration of the cellulose network (Fig. 6b, c). Similarly, Wu et al. (2014) also reported with AgNPs composites BBC that showed a group of absorption bands at 1600 cm^{-1}. Further, these modified membranes showed similar characteristic bands appeared between 1648 and 1084 cm^{-1}, which were comparable to those reported by Rouabhia et al. (2014) and Tabaii et al. (2017).

The results suggested that the CBC-BBC membrane exhibited new characteristic bands appeared at 1668 cm^{-1}-anhydride (C═O stretching, 1534 and 1429 cm^{-1}-aromatic (C—C stretching), 1371, 1336, and 1280 cm^{-1}-Primary alcohol (C—O stretching), and 899 cm^{-1} Alkene (═C—H bending) (Table 1), which did not appear in other modified membranes. Overall all treated membranes showed consistently C═O vibrations of the carboxylate anion particularly at 1668 cm^{-1} when compared to the pure BBC membrane (Fig. 6d) and thus could explain the reduction of Ag^{+} to zero valence metals (Ag^{0}) during the preparation of different BBC membranes, in agreement with Ifuku et al. (2009).

The results of membrane disc diffusion assay (Fig. 7) showed that all the modified membranes independently displayed a bactericidal

Table 3
Comparison of quantitative antimicrobial activity assay of different modified silver based BBC membranes against seven threatening aquatic pathogens.

Pathogens	[#]CC-BBC membrane			[£]BC-BBC membrane			[¶]CBC-BBC membrane		
	Bactericidal activity	Bacteriostatic activity	Killing ratio	Bactericidal activity	Bacteriostatic activity	Killing ratio	Bactericidal activity	Bacteriostatic activity	Killing ratio
	log reduction		%	log reduction		%	log reduction		%
Vibrio harveyi	1.31 ± 0.02[c]	0.89 ± 0.01[c]	87.15 ± 0.44[c]	2.23 ± 0.01[b]	1.81 ± 0.01[b]	98.44 ± 0.02[b]	2.91 ± 0.03[a]	2.48 ± 0.03[a]	99.67 ± 0.02[a]
Vibrio parahaemolyticus	1.32 ± 0.02[c]	1.24 ± 0.01[c]	94.19 ± 0.13[c]	2.27 ± 0.01[b]	2.19 ± 0.01[b]	99.35 ± 0.02[b]	2.93 ± 0.01[a]	2.85 ± 0.04[a]	99.86 ± 0.01[a]
Vibrio alginolyticus	1.35 ± 0.02[c]	1.16 ± 0.01[c]	93.12 ± 0.10[b]	2.35 ± 0.05[b]	2.16 ± 0.03[b]	99.30 ± 0.05[a]	2.50 ± 0.03[a]	2.31 ± 0.02[a]	99.51 ± 0.02[a]
Vibrio vulnificus	2.03 ± 0.03	1.89 ± 0.01	98.72 ± 0.04	2.30 ± 0.73	1.89 ± 0.68	97.83 ± 2.47	2.89 ± 0.13	2.76 ± 0.09	99.82 ± 0.04
Aeromonas hydrophila	1.10 ± 0.08[b]	1.04 ± 0.01[b]	90.91 ± 0.18[c]	1.21 ± 0.09[b]	1.16 ± 0.02[b]	93.04 ± 0.26[b]	1.85 ± 0.20[a]	1.79 ± 0.13[a]	98.34 ± 0.48[a]
Aeromonas veronii	1.30 ± 0.01[c]	1.13 ± 0.06[b]	92.49 ± 0.95[c]	1.54 ± 0.05[b]	1.36 ± 0.02[b]	95.68 ± 0.21[b]	1.97 ± 0.02[a]	1.80 ± 0.09[a]	98.39 ± 0.32[a]
Streptococcus iniae	1.20 ± 0.06[b]	1.07 ± 0.03[b]	91.56 ± 0.56[b]	1.23 ± 0.01[b]	1.10 ± 0.07[b]	92.08 ± 1.28[b]	1.52 ± 0.03[a]	1.39 ± 0.05[a]	95.93 ± 0.49[a]

Data are presented as means SD ± standard error of the mean (*SEM*). Superscripts lower case letter donates significant differences between the treated BBC membranes. Data were analyzed by one way ANOVA. The level of significance was $P \leq .05$.

[#] CC-BBC membrane (TEMPO-oxidized BBC membrane coated with AgNPs).
[£] BC-BBC membrane (BBC membrane coated with bacterial-based AgNPs).
[¶] CBC-BBC membrane (TEMPO-oxidized BBC membrane coated with bacterial-based AgNPs).
[a] represent the High value
[b] Medium
[c] Low

activity due to their unique physical properties, AgNPs-holding capacity, and possible degenerative effects on bacterial cells, in agreement with Pal et al. (2017). Specifically, the CBC-BBC membrane demonstrated effective bactericidal activity compared to others and displayed wide inhibition zones (mm) against all tested pathogens (Table 2).

Moreover, the quantitative assay for antimicrobial activity of different composites was evaluated using antibacterial log reduction assay (Table 3). Generally, the antimicrobial activity was classified according to the log reduction number, where 1-log reduction was considered low, whereas between 1 and 3 and greater than 3-log reduction were considered moderate and high, respectively (Gallant-Behm et al., 2005). As indicated, all treated BBC membranes showed moderate to high antimicrobial effects against all tested pathogens with a log reduction above 1, in agreement with Yang et al. (2012). There was a significant increase in bacteriostatic log-reduction numbers (1.39 ± 0.05 to 2.85 ± 0.04) and killing ratios (95.93 ± 0.49 to 99.86 ± 0.01%) observed with CBC-BBC membrane against all pathogens suggesting that the membrane has more potential than other BBC membranes. A possible explanation is that the physical and mechanical properties of the developed CBC-BBC film, including low pore size and large surface exposure area, may fortify the passage of AgNPs across the membrane and encourage the release of Ag^+ into the external environment, thus favoring a stronger antibacterial effect (Pal et al., 2017).

The potential AgNPs, produced by secondary metabolites of *Pseudomonas* sp. may react effectively, and are attached firmly to oxidized carboxyl groups of BBC membranes and thus increase their antibacterial activities. Similarly, Feng et al. (2014) and Elayaraja et al. (2017) were reported a strong bactericidal activity against several field pathogens using chemical and biological composite BBC membranes either *in vitro* or *in vivo*. Moreover, Rouabhia et al. (2014) investigated about the antibacterial properties of potential guest NPs composite BBC against several multidrug-resistant pathogens suggested that the NPs act as a barrier that reduced the growth of these pathogens and prevent the infection.

Recently, the potential use of nanocomposites for water treatment, including water purification and removal of toxic ions, organic impurities, microbes and their by-products, has attracted keen interest from researchers, especially in the field of aquaculture (Sharma et al., 2011; Yaqoob et al., 2020). Several studies distinctly reported the functional use of nanoparticles and/or nanocomposites for the processing of marine and freshwater fish polyculture with zero water exchange, no oxygen, and high survival rate for eight closed months (Handy, 2012; Bhattacharyya et al., 2015). Moreover, nanocomposites, especially silver, inhibit the growth of water bacteria and common pathogens, keeping the water clean for long-term use (Dankovich and Gray, 2011). Our future goal is to modify the design nanocomposites membrane into a powder form or into a nano-bio-bag unified filter, to be easily amenable for the processing of fish and shrimp culture water.

In conclusion, the BBC membranes are unique versatile material with extraordinary physicochemical properties and good bioavailability. The CC-BBC membrane tends to retain high chemical residues of toxic and carcinogenic properties, which may hinder its field application. The novel CBC-BBC membrane exhibited high bactericidal and bacteriostatic activities as well as high killing ratios against the selected aquatic pathogens. Finally, yet importantly, the current data provide an insight into the potential use of bacterial-based AgNPs in aquaculture as a surrogate for many classical antibiotics to overcome the problem of antibiotic resistance. Nonetheless, their field application and validation to combat pathogens still require further investigation.

Data availability

The authors declare that they do not have any shared data available.

Author contributions

S.E., S.Z., and C.R conceived and designed the experiments. E.S., M.M., and Y.Z performed the experiments. L.G., Z. K., and M. G. analyzed the data and drafted the manuscript; E.S., M.M., S.Z., and C.R. writing, review and editing. All authors have read and agreed to the published version of the manuscript.

Declaration of Competing Interest

The authors declare that there are no conflicts of interest.

Acknowledgements

This work was supported by the Key R&D Program of the Ministry of Science and Technology of China (Grant No. 2017YFD0701703), the Key Program of Science and Technology of Zhejiang Province (Grant No. 2019C02084), and the Second Century Fund (C2F, Batch 3/2019), Chulalongkorn University, Thailand.

Appendix A. Supplementary data

Supplementary data to this article can be found online at https://doi.org/10.1016/j.aquaculture.2020.735746.

References

Abdel Rahim, K., Mahmoud, S.Y., Ali, A.M., Almaary, K.S., Mustafa, A.E.-Z.M., Husseiny, S.M., 2017. Extracellular biosynthesis of silver nanoparticles using *Rhizopus stolonifer*. Saudi J. Biol. Sci. 24, 208–216.

Adepu, S., Khandelwal, M., 2018. Broad-spectrum antimicrobial activity of bacterial cellulose silver nanocomposites with sustained release. J. Mater. Sci. 53, 1596–1609.

Agnew, W., Barnes, A.C., 2007. *Streptococcus iniae*: an aquatic pathogen of global veterinary significance and a challenging candidate for reliable vaccination. Vet. Microbiol. 122 (1–2), 1–15.

Algammal, A.M., Mohamed, M.F., Tawfiek, B.A., Hozzein, W.N., El Kazzaz, W.M., Mabrok, M., 2020. Molecular typing, antibiogram and pcr-rflp based detection of *Aeromonas hydrophila* complex isolated from *Oreochromis niloticus*. Pathogens. 9 (3), 238.

Austin, B., 2019. Methods for the diagnosis of bacterial fish diseases. Mar. Life Sci. Technol. 1, 41–49.

Balashanmugam, P., Kalaichelvan, P.T., 2015. Biosynthesis characterization of silver nanoparticles using *Cassia roxburghii* DC. aqueous extract, and coated on cotton cloth for effective antibacterial activity. Int. J. Nanomedicine 10, 87.

Bernal, M.G., Marrero, R.M., Campa-Córdova, Á.I., Mazón-Suástegui, J.M., 2017. Probiotic effect of Streptomyces strains alone or in combination with Bacillus and lactobacillus in juveniles of the white shrimp *Litopenaeus vannamei*. Aquac. Int. 25, 927–939.

Bhattacharyya, A., Reddy, S., Hasan, M., Adeyemi, M., Marye, R., 2015. Nanotechnology-a unique future technology in aquaculture for the food security. Int. J. Bioassays. 4, 4115–4126.

Cao, X., Ding, B., Yu, J., Al-Deyab, S.S., 2013. In situ growth of silver nanoparticles on TEMPO-oxidized jute fibers by microwave heating. Carbohydr. Polym. 92, 571–576.

Chen, M., Kang, H., Gong, Y., Guo, J., Zhang, H., Liu, R., 2015. Bacterial cellulose supported gold nanoparticles with excellent catalytic properties. ACS Appl. Mater. Interfaces 7 (39), 21717–21726.

Dahoumane, S.A., Wijesekera, K., Filipe, C.D., Brennan, J.D., 2014. Stoichiometrically controlled production of bimetallic gold-silver alloy colloids using micro-alga cultures. J. Colloid Interface Sci. 416, 67–72.

Dankovich, T.A., Gray, D.G., 2011. Bactericidal paper impregnated with silver nanoparticles for point-of-use water treatment. Environ. Sci. Technol. 45, 1992–1998.

Dong, H.T., Techatanakitarnan, C., Jindakittikul, P., Thaiprayoon, A., Taengphu, S., Charoensapsri, W., Khunrae, P., Rattanarojpong, T., Senapin, S., 2017. *Aeromonas jandaei* and *Aeromonas veronii* caused disease and mortality in Nile tilapia, *Oreochromis niloticus* (L.). J. Fish Dis. 40 (10), 1395–1403.

Elayaraja, S., Zagorsek, K., Li, F., Xiang, J., 2017. In situ synthesis of silver nanoparticles into TEMPO-mediated oxidized bacterial cellulose and their antivibriocidal activity against shrimp pathogens. Carbohydr. Polym. 166, 329–337.

El-Sayed, M., Algammal, A., Abouel-Atta, M., Mabrok, M., Emam, A., 2019. Pathogenicity, genetic typing, and antibiotic sensitivity of *Vibrio alginolyticus* isolated from *Oreochromis niloticus* and Tilapia zillii. Rev. Med. Vet. 170, 80–86.

Feng, J., Shi, Q., Li, W., Shu, X., Chen, A., Xie, X., Huang, X., 2014. Antimicrobial activity of silver nanoparticles in situ growth on TEMPO-mediated oxidized bacterial cellulose. Cellulose. 21, 4557–4567.

Fondevila, M., 2010. Potential use of silver nanoparticles as an additive in animal feeding. In: Silver Nanoparticles. Rijeka, Croatia: InTech, pp. 325–334.

Food and Agriculture Organization of the United Nations (FAO), 2018. Fishery and aquaculture statistics. Global aquaculture production 1950–2016 (FishstatJ). In: FAO Fisheries and Aquaculture Department [online]. Rome. Updated 2018.

Gallant-Behm, C.L., Yin, H.Q., Liu, S., Heggers, J.P., Langford, R.E., Olson, M.E., Hart, D.A., Burrell, R.E., 2005. Comparison of in vitro disc diffusion and time kill-kinetic assays for the evaluation of antimicrobial wound dressing efficacy. Wound Repair Regen. 13, 412–421.

Gholipourkanani, H., Buller, N., Lymbery, A., 2019. *In vitro* antibacterial activity of four nano-encapsulated herbal essential oils against three bacterial fish pathogens. Aquac. Res. 50, 871–875.

Gutierrez, J., Fernandes, S.C., Mondragon, I., Tercjak, A., 2013. Multifunctional hybrid nanopapers based on bacterial cellulose and sol–gel synthesized titanium/vanadium oxide nanoparticles. Cellulose. 20 (3), 1301–1311.

Handy, R., 2012. FSBI briefing paper: nanotechnology in fisheries and aquaculture. Fish. Soc. Br. Isles 1–29.

Hu, W., Chen, S., Li, X., Shi, S., Shen, W., Zhang, X., Wang, H., 2009. In situ synthesis of silver chloride nanoparticles into bacterial cellulose membranes. Mater. Sci. Eng. C 29 (4), 1216–1219.

Ifuku, S., Tsuji, M., Morimoto, M., Saimoto, H., Yano, H., 2009. Synthesis of silver nanoparticles templated by TEMPO-mediated oxidized bacterial cellulose nanofibers. Biomacromolecules. 10, 2714–2717.

Jinga, S., Isopencu, G., Stoica-Guzun, A., Stroescu, M., Ferdes, M., Ohreac, B., 2013. Silver green synthesis on bacterial cellulose membranes using tannic acid. Dig. J. Nanomater. Biostruct. 8, 1711–1717.

Jun, S.-H., Park, S.-G., Kang, N.-G., 2019. One-pot method of synthesizing TEMPO-oxidized bacterial cellulose nanofibers using immobilized TEMPO for skincare applications. Polymers. 11, 1044.

Khamrai, M., Banerjee, S.L., Kundu, P.P., 2017. Modified bacterial cellulose based self-healable polyeloctrolyte film for wound dressing application. Carbohydr. Polym. 174, 580–590.

Khan, S., Ul-Islam, M., Ullah, M.W., Kim, Y., Park, J.K., 2015. Synthesis and characterization of a novel bacterial cellulose–poly (3, 4-ethylenedioxythiophene)–poly (styrene sulfonate) composite for use in biomedical applications. Cellulose. 22, 2141–2148.

Kumar, S., Mukherjee, A., Dutta, J., 2020. Chitosan based nanocomposite films and coatings: emerging antimicrobial food packaging alternatives. Trends Food Sci. Technol. 97, 196–209.

Lai, C., Zhang, S., Chen, X., Sheng, L., 2014. Nanocomposite films based on TEMPO-mediated oxidized bacterial cellulose and chitosan. Cellulose. 21, 2757–2772.

Li, W.-R., Xie, X.-B., Shi, Q.-S., Zeng, H.-Y., You-Sheng, O.-Y., Chen, Y.-B., 2010. Antibacterial activity and mechanism of silver nanoparticles on *Escherichia coli*. Appl. Microbiol. Biotechnol. 85, 1115–1122.

Lightner, D.V., 1985. A review of the diseases of cultured penaeid shrimps and prawns with emphasis on recent discoveries and developments. In: Proceedings of the First International Conference on the Culture of Penaeid Prawns/Shrimps, 4–7 December 1984, Iloilo City, Philippines. Aquaculture Department, Southeast Asian Fisheries Development Center, pp. 79–103.

Loh, E.Y.X., Mohamad, N., Fauzi, M.B., Ng, M.H., Ng, S.F., Amin, M.C.I.M., 2018. Development of a bacterial cellulose-based hydrogel cell carrier containing keratinocytes and fibroblasts for full-thickness wound healing. Sci. Rep. 8, 1–12.

Mabrok, M., Machado, M., Serra, C., Afonso, A., Valente, L., Costas, B., 2016. Tenacibaculosis induction in the Senegalese sole (*Solea senegalensis*) and studies of Tenacibaculum maritimum survival against host mucus and plasma. J. Fish Dis. 39, 1445–1455.

Mandal, D., Bolander, M.E., Mukhopadhyay, D., Sarkar, G., Mukherjee, P., 2006. The use of microorganisms for the formation of metal nanoparticles and their application. Appl. Microbiol. Biotechnol. 69, 485–492.

Mijnendonckx, K., Leys, N., Mahillon, J., Silver, S., Van Houdt, R., 2013. Antimicrobial silver: uses, toxicity and potential for resistance. Biometals. 26, 609–621.

Mitiku, A.A., Yilma, B., 2018. A review on green synthesis and antibacterial activity of silver nanoparticles. Int. J. Pharm. Sci. Rev. Res. 46, 52–57.

Nelson, D., Priscyla, D., Oswaldo, L., Gabriel, I., Elisa, E., 2005. Mechanical aspects of biosynthesis of silver nanoparticles by several *Fusarium oxysporum* strains. J. Nanobiotechnol. 3, 8.

Oliveira, J.M., Carvalho, L., Silva-Correia, J., Vieira, S., Majchrzak, M., Lukomska, B., Stanaszek, L., Strymecka, P., Malysz-Cymborska, I., Golubczyk, D., 2018. Hydrogel-based scaffolds to support intrathecal stem cell transplantation as a gateway to the spinal cord: clinical needs, biomaterials, and imaging technologies. NPJ Regen. Med. 3, 1–9.

Pal, S., Nisi, R., Stoppa, M., Licciulli, A., 2017. Silver-functionalized bacterial cellulose as antibacterial membrane for wound-healing applications. ACS Omega. 2, 3632–3639.

Pinto, R.J., Marques, P.A., Neto, C.P., Trindade, T., Daina, S., Sadocco, P., 2009. Antibacterial activity of nanocomposites of silver and bacterial or vegetable cellulosic fibers. Acta Biomater. 5, 2279–2289.

Pourali, P., Yahyaei, B., Ajoudanifar, H., Taheri, R., Alavi, H., Hoseini, A., 2014. Impregnation of the bacterial cellulose membrane with biologically produced silver nanoparticles. Curr. Microbiol. 69, 785–793.

Rahman, A., Kumar, S., Bafana, A., Dahoumane, S.A., Jeffryes, C., 2019. Biosynthetic conversion of Ag^{+} to highly stable Ag^{0} nanoparticles by wild type and cell wall deficient strains of Chlamydomonas reinhardtii. Molecules. 24, 98.

Rajwade, J., Paknikar, K., Kumbhar, J., 2015. Applications of bacterial cellulose and its composites in biomedicine. Appl. Microbiol. Biotechnol. 99, 2491–2511.

Rouabhia, M., Asselin, J.R.M., Tazi, N., Messaddeq, Y.S., Levinson, D., Zhang, Z., 2014. Production of biocompatible and antimicrobial bacterial cellulose polymers functionalized by RGDC grafting groups and gentamicin. ACS Appl. Mater. Interfaces 6, 1439–1446.

Saha, N., Gupta, S.D., 2017. Low-dose toxicity of biogenic silver nanoparticles fabricated

by *Swertia chirata* on root tips and flower buds of *Allium cepa*. J. Hazard. Mater. 330, 18–28.
Schenk, R.U., Hildebrandt, A., 1972. Medium and techniques for induction and growth of monocotyledonous and dicotyledonous plant cell cultures. Can. J. Bot. 50, 199–204.
Shabnam, N., Pardha-Saradhi, P., 2013. Photosynthetic electron transport system promotes synthesis of Au-nanoparticles. PLoS One 8.
Sharma, M.R., Aklakur, M., Ahmad, S., Kumar, N., Khan, M., Ramya, V., 2011. Nanotechnology: a novel tool for aquaculture and fisheries development. A prospective mini-review. Fish. Aquac. J. 1–6.
Singh, P., Kim, Y.J., Singh, H., Wang, C., Hwang, K.H., Farh, M.E.-A., Yang, D.C., 2015. Biosynthesis, characterization, and antimicrobial applications of silver nanoparticles. Int. J. Nanomedicine 10, 2567.
Singh, H., Du, J., Singh, P., Yi, T.H., 2018. Extracellular synthesis of silver nanoparticles by Pseudomonas sp. THG-LS1. 4 and their antimicrobial application. J. Pharm. Anal. 8, 258–264.
Sivaramasamy, E., Zhiwei, W., Li, F., Xiang, J., 2016. Enhancement of vibriosis resistance in Litopenaeus vannamei by supplementation of biomastered silver nanoparticles by *Bacillus subtilis*. J. Nanomed. Nanotechnol. 7, 2.
Surachetpong, W., Janetanakit, T., Nonthabenjawan, N., Tattiyapong, P., Sirikanchana, K., Amonsin, A., 2017. Outbreaks of tilapia lake virus infection, Thailand, 2015–2016. Emerg. Infect. Dis. 23, 1031.
Tabaii, M.J., Etemadzade, S., Emtiazi, G., 2017. Biosynthesis, characterization and optical properties of nano-crystalline rosette-shape aragonite and iron (III) chloride–graphite intercalated materials from bacterial cellulose. J. Mater. Sci. Mater. Electron. 28, 8339–8346.
Toranzo, A.E., Magariños, B., Romalde, J.L., 2005. A review of the main bacterial fish diseases in mariculture systems. Aquaculture. 246, 37–61.
Vanaraj, S., Keerthana, B.B., Preethi, K., 2017. Biosynthesis, characterization of silver nanoparticles using quercetin from *Clitoria ternatea* L to enhance toxicity against bacterial biofilm. J. Inorg. Organomet. Polym. Mater. 27, 1412–1422.
Vasantharaj, S., Sathiyavimal, S., Saravanan, M., Senthilkumar, P., Gnanasekaran, K., Shanmugavel, M., Manikandan, E., Pugazhendhi, A., 2019. Synthesis of ecofriendly copper oxide nanoparticles for fabrication over textile fabrics: characterization of antibacterial activity and dye degradation potential. J. Photochem. Photobiol. B Biol. 191, 143–149.
Velmurugan, P., Iydroose, M., Mohideen, M.H.A.K., Mohan, T.S., Cho, M., Oh, B.-T., 2014. Biosynthesis of silver nanoparticles using Bacillus subtilis EWP-46 cell-free extract and evaluation of its antibacterial activity. Bioprocess Biosyst. Eng. 37, 1527–1534.
Wahdan, A., Fadel, A., Mabrok, M., 2020. New insights into the effect of Origanum extracts on the gene expression profiles of multidrug-resistant isolates of *Pseudomonas aeruginosa* retrieved from *Oreochromis niloticus*. Turk. J. Fish. Aquat. Sci. 7, 507–519.
Wan, Y., Hong, L., Jia, S.R., Huang, Y., Zhu, Y., Wang, Y.L., Jiang, H.J., 2006. Synthesis and characterization of hydroxyapatite–bacterial cellulose nanocomposites. Compos. Sci. Technol. 66, 1825–1832.
Wasim, M., Khan, M.R., Mushtaq, M., Naeem, A., Han, M., Wei, Q., 2020. Surface modification of bacterial cellulose by copper and zinc oxide sputter coating for UV-resistance/antistatic/antibacterial characteristics. Coatings. 10 (4), 364.
Wu, J., Zheng, Y., Song, W., Luan, J., Wen, X., Wu, Z., Chen, X., Wang, Q., Guo, S., 2014. In situ synthesis of silver-nanoparticles/bacterial cellulose composites for slow-released antimicrobial wound dressing. Carbohydr. Polym. 102, 762–771.
Xiu, Z.M., Zhang, Q.B., Puppala, H.L., Colvin, V.L., Alvarez, P.J., 2012. Negligible particle-specific antibacterial activity of silver nanoparticles. Nano Lett. 12, 4271–4275.
Xu, C., Kuang, H., Xu, L., 2019. Pathogen Immunoassay in Food, Food Immunoassay. Springer, pp. 255–319.
Yang, G., Xie, J., Hong, F., Cao, Z., Yang, X., 2012. Antimicrobial activity of silver nanoparticle impregnated bacterial cellulose membrane: effect of fermentation carbon sources of bacterial cellulose. Carbohydr. Polym. 87, 839–845.
Yaqoob, A.A., Parveen, T., Umar, K., Mohamad Ibrahim, M.N., 2020. Role of nanomaterials in the treatment of wastewater: a review. Water 12 (2), 495.
Zhang, X., He, X., Austin, B., 2020. *Vibrio harveyi*: a serious pathogen of fish and invertebrates in mariculture. Mar. Life Sci. Technol. https://doi.org/10.1007/s42995-020-00037-z.